Structure–Property Relationships in Elastomeric Carboxy-Telechelic Polyisoprene Ionomers Neutralized with Divalent Cations

Richard A. Register,[†] Marianne Foucart,[‡] Robert Jérôme,[‡] Y. Samuel Ding,[†,§] and Stuart L. Cooper*[†]

Department of Chemical Engineering, University of Wisconsin—Madison, Madison, Wisconsin 53706, and Laboratoire de Chimie Macromoléculaire et de Catalyse Organique, Universite de Liège, Sart-Tilman, Liège, Belgium. *Received August 20, 1987*

ABSTRACT: A series of narrow molecular weight distribution carboxy-telechelic vinyl polyisoprenes of molecular weight 8000, neutralized with Ca^{2+}, Sr^{2+}, Ni^{2+}, Zn^{2+}, and Cd^{2+}, are examined by several techniques. The small-strain tensile moduli of these materials are found to be significantly higher than predicted on the basis of the contribution of ionic aggregates acting as physical cross-links and fillers, with the Ca^{2+} and Sr^{2+} ionomers having the highest moduli. The modulus enhancement is attributed to entanglements, in the form of interlocking loops formed when both ends of a telechelic chain reside in the same aggregate. Small-angle X-ray scattering reveals that the Ca^{2+} and Sr^{2+} materials have larger aggregates and therefore more trapped entanglements and higher moduli. Strain-hardening behavior is observed for the Ca^{2+} and Ni^{2+} telechelics, but not in the other three materials. Extended X-ray absorption fine structure spectroscopy shows that these two materials have more ordered ionic microdomains, making ion hopping more difficult. The Ca^{2+} and Ni^{2+} telechelics strain-harden and break when the interlocking loops pull taut, whereas stressed entanglements in the other telechelics can relax by pulling ionic chain ends out of the aggregates.

I. Introduction

Copolymers containing less than 10 mol % ionic comonomer, termed ionomers, form a class of theoretically interesting and commercially important materials. The minority comonomer typically contains a carboxylic or sulfonic acid group, and upon neutralization of the acid groups with a metal salt, the material properties often change dramatically. Marked increases in modulus, adhesive strength, tear and abrasion resistance, melt viscosity, and impact strength have been reported.[1-5] It has been proposed,[6,7] and by now generally accepted, that these effects result from aggregation of the ions into microdomains, which act as physical cross-links in the material.

In most ionomers, the ionic groups are spaced randomly along a high molecular weight polymer chain. In contrast, there has recently been strong interest in telechelic ionomers, which are low molecular weight polymers containing ionic groups only at the ends. While early studies focused on salts of polydisperse linear polybutadiene terminated with carboxylate groups,[8-10] more recent investigations have concentrated on specially tailored telechelics produced by anionic or cationic techniques. Examples include the three-arm star sulfonated polyisobutylenes of Kennedy et al.[11-13] and the linear narrow molecular weight distribution carboxy-telechelic polyisoprenes of Jérôme et al.[10,14-16] Williams et al.[17] examined the small-angle X-ray scattering (SAXS) patterns for several carboxy-telechelic polyisoprenes and noted the extremely sharp phase separation between the ionic domains and the polyisoprene matrix. Tant et al.[18] examined the tensile properties of Al^{3+}, Ba^{2+}, and Zr^{4+} salts of carboxy-telechelic polyisoprenes over the molecular weight range 15000–45000 and concluded that both the cation and the molecular weight played important roles in the behavior of the materials. In this investigation, we examine elastomers prepared from a carboxy-telechelic polyisoprene of molecular weight 8000, neutralized with five divalent cations: Ca^{2+}, Sr^{2+}, Ni^{2+}, Zn^{2+}, and Cd^{2+}.

* Author to whom correspondence should be addressed.
† University of Wisconsin—Madison.
‡ Laboratoire de Chimie Macromoléculaire et de Catalyse Organique.
§ Present address: Baxter Healthcare, Inc., Round Lake, IL 60073.

II. Experimental Section

A. Synthesis. The synthesis of carboxy-telechelic polyisoprenes has been described previously.[15-17] The polymerization was carried out in tetrahydrofuran at −78 °C, with sodium naphthalide as initiator. A small amount of α-methylstyrene monomer, approximately two to three units per living end, was added after completion of the isoprene polymerization to reduce the reactivity of the chain ends, which were then terminated by the addition of gaseous CO_2. The resulting sodium carboxylate end groups were converted to carboxylic acid by the addition of HCl. The polymers were then precipitated 3 times in methanol. The functionality of these polymers is 1.90, as determined by potentiometric titration of the acid end groups with tetramethylammonium hydroxide in toluene/methanol solution (90/10 v/v). The molecular weight was determined by gel permeation chromatography using a Waters 200, with the polymer dissolved in tetrahydrofuran at 25 °C. By use of polystyrene calibration standards and the universal calibration curve, the molecular weight was found to be 8000 g/mol.

Neutralization was accomplished by the addition of the metal methoxide (Ca, Sr) or acetate (Ni, Zn, Cd) in toluene solution, using 95% of the stoichiometric amount of neutralizing agent to avoid the precipitation of excess neutralizing agent in the ionomer. The methanol or acetic acid byproduct was removed by azeotropic distillation. Finally, approximately 1% by weight of the antioxidant Irganox 1010 was added to prevent chemical cross-linking of the polyisoprene units. The materials were then dried at 25 °C at 10^{-2} Torr to constant weight. Specimens for testing were compression-molded for 5 min at 70 °C into sheets approximately 0.5 mm thick or disks approximately 2 mm thick. All samples were stored in a desiccator over $CaSO_4$ until use.

B. Instrumental Conditions. The proton Fourier transform nuclear magnetic resonance (^{1}H FTNMR) spectra were acquired on a Bruker WP-200 at 200.13 MHz. Approximately 5 mg of sample was dissolved in 0.5 mL of $CDCl_3$. Thirty-two coadded scans were used, with a pulse width of 1.4 μs and no delay time.

Differential scanning calorimetry (DSC) thermograms were collected over the range −120 to 220 °C on a Perkin-Elmer DSC-II interfaced to a TADS data station. The heating rate was 20 °C/min; indium and mercury were used as calibration standards. The sample weights used were 14 ± 4 mg.

Dogbone samples for tensile testing were stamped out with a standard ASTM D1708 die. Measurements were performed in air, at 30 °C, on an Instron TM at a crosshead speed of 0.5 in./min. All reported data are the average of three tests.

The small-angle X-ray scattering (SAXS) experiments were performed with an Elliot GX-21 rotating anode X-ray generator operated with a copper target at 40-kV accelerating potential and 15-mA emission current. Cu Kα X-rays were selected by filtering

0024-9297/88/2221-1009$01.50/0

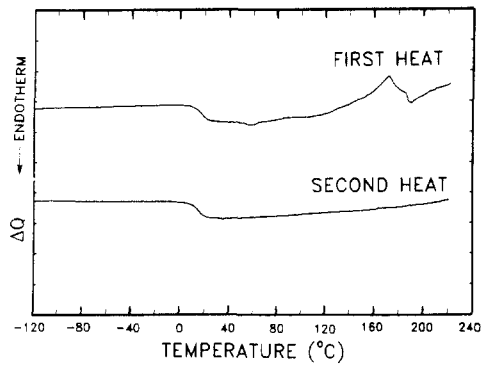

Figure 1. DSC traces for carboxy-telechelic polyisoprene (M = 8000) neutralized with Sr^{2+}. The upper trace was obtained on a sample quenched from room temperature and heated; this was then quenched and heated again to give the lower trace.

with nickel foil and by pulse-height analysis at the detector. An Anton-Paar compact Kratky camera was used to collimate the X-rays into a line measuring 1.00 cm × 100 μm. The scattered X-rays were detected with a TEC 211 linear position sensitive detector, positioned at a sample-to-detector distance of 60 cm for a q range ($q = (4\pi \sin\theta)/\lambda$) of 0.15–5.4 nm^{-1}. The data were corrected for detector sensitivity, dark current, empty beam scattering, and sample absorption and placed on an absolute intensity scale by comparison with a calibrated Lupolen polyethylene standard.[19]

The transmission extended X-ray absorption fine structure (EXAFS) spectra were collected on the A-2, C-1, and C-2 stations of the Cornell High Energy Synchrotron Source (CHESS). Data reduction followed a standard procedure of preedge and postedge background removal, extraction of the EXAFS oscillations $\chi(k)$, Fourier transformation of $\chi(k)$, and finally application of an inverse transform to isolate the EXAFS contribution from a selected region in real space.[20-22]

III. Results and Discussion

A. NMR Analysis of Diene Microstructure. As all the ionomers were prepared from the same telechelic carboxylic acid, only the Ca^{2+} salt was examined. Peak assignments were based on previous results of Bovey[23] and Pham.[24] The vinylene peak of the 3,4 microstructural units was observed as a resolved multiplet (at δ = 5.7 ppm relative to tetramethylsilane), while the vinyl protons of the 1,2 and 3,4 units gave rise to overlapping peaks (at 4.84 and 4.63 ppm, respectively). No peaks were observed near 5.1 ppm, the resonance of the vinylene proton in 1,4 units. On the basis of peak areas, the microstructure consists of 59% 3,4 addition, 41% 1,2 addition, and no 1,4 addition. These values are comparable to those (65/35 of 3,4/1,2) reported earlier for the isoprene polymerization initiated by sodium α-methylstyrene tetramer.[15]

B. Differential Scanning Calorimetry (DSC). Typical DSC results are shown in Figure 1, for the Sr^{2+} neutralized material. The upper curve is the trace obtained by quenching the sample to −120 °C at the nominal rate of 320 °C/min and then scanning. After the first scan, the sample was again quenched at 320 °C/min to −120 °C and the scan repeated.

The glass transition of the polyisoprene matrix is visible at 19 °C in both scans. In the first scan, above 150 °C, there is also what appears to be a broad exotherm followed by an endotherm. Whatever processes are responsible for this feature are apparently complete at the end of the first scan, since this region of the second scan is smooth. Similar features were observed in the first DSC scans of all samples, regardless of cation. A high-temperature endotherm has also been noted in DSC data for telechelic poly(α-methylstyrene) ionomers,[25] but at present its origin is not clear. The glass transitions of the materials, taken as the midpoints, lay within the narrow range 15–19 °C regardless of cation.

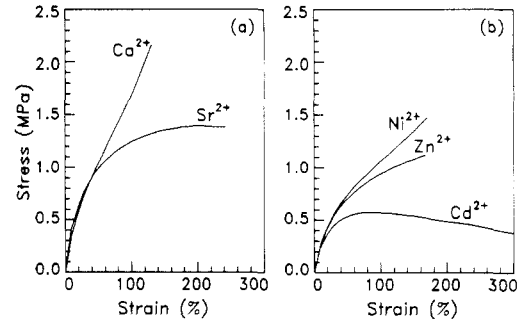

Figure 2. Stress–strain behavior of carboxy-telechelic polyisoprenes (M = 8000): (a) Ca^{2+} and Sr^{2+} telechelics; (b) Ni^{2+}, Zn^{2+}, and Cd^{2+} telechelics.

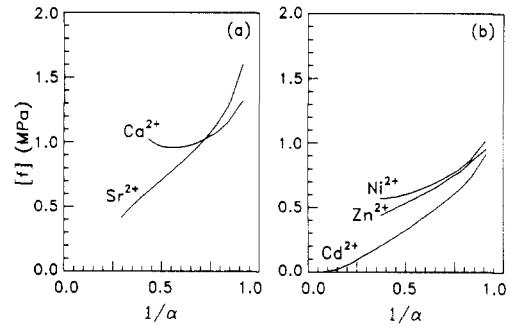

Figure 3. Data of Figure 3 replotted in the Mooney–Rivlin format: (a) Ca^{2+} and Sr^{2+} telechelics; (b) Ni^{2+}, Zn^{2+}, and Cd^{2+} telechelics.

C. Tensile Measurements. Stress–strain curves are shown in Figure 2 for all five materials, where differences between the materials neutralized with different cations can be clearly seen. Figure 2a shows the materials neutralized with the alkaline earth cations Ca^{2+} and Sr^{2+}, while those neutralized with the transition-metal cations Ni^{2+}, Zn^{2+}, and Cd^{2+} are shown in Figure 2b. The shapes and scales of these curves are generally similar to those measured by Tant et al.[18] Note that the Cd^{2+} ionomer actually extended well beyond 300% elongation, to approximately 1600%, and exhibited essentially no recovery upon breaking. The Ca^{2+} and Ni^{2+} materials, by contrast, snapped back to within 40% of their unstressed length after breaking. The Zn^{2+} and Sr^{2+} telechelics exhibited intermediate behavior.

In order to quantitate these tensile measurements, the data were recast in the form

$$[f] = \tau/(\alpha - 1/\alpha^2) \quad (1)$$

where $[f]$ is termed the reduced stress, τ is the engineering stress, and α is the ratio of stressed to unstressed sample length. As originally noted by Mooney[26] and Rivlin,[27] tensile data for many chemically cross-linked elastomers[28] lie on straight lines when plotted as $[f]$ vs $1/\alpha$. The Mooney–Rivlin plots for the telechelics are shown in Figure 3 and are clearly not straight lines. A major difference between chemically cross-linked elastomers and ionomers is that the former, for the most part, are time-independent materials; that is, the cross-links are stable throughout the test. In ionomers, the cross-links are physical, rather than chemical, and may be subject to disruption by applied stress. The large permanent sets observed for these materials indicate that such an "ion-hopping" mechanism[29-31] must be operating. Tant et al.[18] arrived at similar conclusions for their telechelic polyisoprene ionomers, based on stress relaxation experiments.

Table I
Zero-Strain Young's Moduli

neutralizing cation	E, MPa	neutralizing cation	E, MPa
Ca^{2+}	1.47	Zn^{2+}	1.07
Sr^{2+}	1.88	Cd^{2+}	1.08
Ni^{2+}	1.23		

Because of the time-dependent nature of these materials, any network parameters obtained from these plots have to be regarded with skepticism. Presenting the data in this form does have two advantages, however. First, it clearly shows the small-strain tensile modulus, which is the $1/\alpha = 1$ intercept of the curves. Inspection of Figure 3 shows that the Ca^{2+} and Sr^{2+} ionomers have higher small-strain moduli than the Ni^{2+}, Zn^{2+}, and Cd^{2+} materials. The data from 10–30% strain were fit to a straight line and extrapolated to zero strain; since this is the short-time and small-strain region of the curves, the time-dependent nature of these ionomers least affects the data here. The modulus values are listed in Table I. The two alkaline earth materials have an average modulus nearly 50% higher than the average of the three transition-metal materials, despite having identical ion contents and molecular weights.

Moreover, these modulus values are higher than the values predicted by rubber elasticity theory, if we consider the effective network elements to be those polyisoprene chains terminated at both ends with metal carboxylate groups. In this case, the tensile modulus E would be given by[32-34]

$$E = 3[(f-2)/f]\nu RT \quad (2)$$

where f is the cross-link functionality, ν is the density of elastically effective chains, R is the gas constant, and T is the absolute temperature. The bracketed quantity reflects the mobility of the cross-links within the matrix. Assuming that all metal carboxylate groups reside within aggregates, that all elastically effective chains have metal carboxylate groups at both ends, and that these ionic groups are randomly distributed among all the chain ends, the ν value for these telechelics is approximately 1.07×10^{-4} mol/cm^3. If we further assume that the functionality of an ionic cross-link is large, such that the bracketed quantity in eq 2 approaches unity, we calculate an upper bound on E equal to 0.81 MPa. The observed values lie in the range 1.07–1.88 MPa, so some factor must be acting to enhance the modulus. Because of the relatively low concentration of ionic groups, the ionic aggregates do not occupy a significant fraction of the materials' volumes, so the filler effect is small; moreover, the volume fraction of ionic aggregates should be nearly the same for all five materials.

Returning to the Mooney–Rivlin plots in Figure 3, we find they also serve to point out an unusual strain-hardening feature (positive deviation from linearity) observed for the Ca^{2+} telechelic near 50% elongation and to a lesser extent for the Ni^{2+} ionomer near 100% elongation. This feature is absent in the other three materials. Such behavior is also apparent in some of the data presented by Tant et al.[18] for 14500 molecular weight telechelic polyisoprenes neutralized with Al^{3+} and Zr^{4+}, although it was not commented on there. In rubbers, strain hardening is often evidence of stress-induced crystallization; however, the NMR results showed these telechelics to be copolymers of the two types of vinyl addition and thus incapable of crystallization. Nor is the strain hardening due to the finite extensibility of the primary chains, of molecular weight 8000. An estimate of the maximum extensibility may be made by approximating the unstressed chains as random coils. By use of the well-known formula[35] for the root mean square end-to-end distance of a random coil $(\bar{r}^2)^{1/2}$, and the expression for the end-to-end distance r in the fully extended, planar zigzag chain, the maximum extension ratio α_{max} is

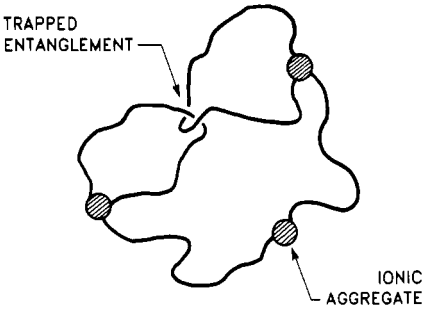

Figure 4. Schematic representation of interlocking loops (trapped entanglements).

$$\alpha_{max} = r/(\bar{r}^2)^{1/2} = \sin(\theta_b/2)(m/C)^{1/2} \quad (3)$$

where θ_b is the angle made by two main-chain bonds and m is the number of main-chain bonds. C, termed the characteristic ratio, is a material-dependent constant increasing with chain stiffness. Due to the unusual microstructure of the polyisoprene chain, no value of C could be found in the literature. However, the repeat units of poly(1-pentene) and poly(methyl acrylate) are sterically similar to those of vinyl polyisoprene and have C values of 9.2 and 8.3, respectively,[36] so a conservative estimate of α_{max} may be obtained with $C = 9$. With a tetrahedral C–C bond angle of 109.5° and $m = 235$ for a pure vinyl polyisoprene chain of 8000 molecular weight, α_{max} is calculated to be 4.2, or 320% extension. While several approximations were made to arrive at this result, the fact that the strain hardening occurs at only 50–100% extension indicates it is not due to the polyisoprene chains approaching their planar zigzag conformations.

Trapped entanglements often contribute appreciably to the moduli of networks formed by chemically cross-linking in bulk.[28] The situation for the telechelic ionomers is somewhat different, since the primary chains are of low molecular weight and would not be expected to be highly entangled. However, entanglements can still form when the ionic groups aggregate, and a large fraction of these are likely to be interlocking "loops", as shown schematically in Figure 4. It has long been recognized[7,37,38] that a large fraction of the ionic sites would, upon ionic aggregation, coalesce into the same aggregate as their topological neighbor. For a linear telechelic ionomer, this corresponds to both ends residing in the same aggregate, creating a "loop" of polymer chain. In bulk, this loop will be entangled with other loops, and as long as the ionic aggregates are not disrupted, these interlocking loops are elastically effective entanglements. As can be visualized from Figure 4, these loops will pull taut at a much lower extension than would be required to fully extend the entire polymer chain.

When these interlocking loops pull taut, one of two effects may result. If the ionic aggregates are highly cohesive and do not rupture, then the polymer chains must break, and the material will snap back to approximately its unstressed length. If the aggregates are weakly cohesive, the stressed entanglements can relax by "ion-hopping", or pulling the ionic groups out of the aggregates.

Two questions remain, however: why is the modulus enhancement, attributed primarily to these interlocking loops, greater for the Ca^{2+} and Sr^{2+} ionomers than for the Ni^{2+}, Zn^{2+}, and Cd^{2+} telechelics, and why is the stress-

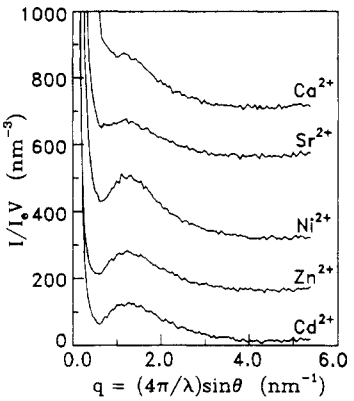

Figure 5. Slit-smeared SAXS patterns for carboxy-telechelic polyisoprenes (M = 8000). Intensities include an arbitrary offset for clarity.

hardening behavior exhibited only by the telechelics neutralized with Ca^{2+} and Ni^{2+}? Small-angle X-ray scattering (SAXS) and extended X-ray absorption fine structure (EXAFS) spectroscopy were employed to address these questions.

D. Small-Angle X-ray Scattering (SAXS). The slit-smeared SAXS patterns for the telechelics are shown in Figure 5, each with an arbitrary intensity offset. Due to the low concentration of ions in these materials, they are poor scatterers, but these curves do show the two features typically found in ionomer SAXS patterns: a peak, seen here from 1.2–1.5 nm^{-1}, and a steep upturn at very low angle. The peak has been considered evidence of ionic aggregation since it was first observed;[6] however, the origin of the low-angle upturn is still in question.[39]

To further analyze the data, it was desmeared according to the method devised by Lake,[40] using an experimentally determined beam intensity profile. The data in the range 3.0–5.0 nm^{-1} were fit to Porod's Law[41] plus a constant background term; this background was then subtracted from the curves. The data were then fit to a modified Yarusso (liquidlike) model,[42] which attributes the peak to interparticle scattering. The ionic aggregates in the Yarusso model have an ionic core radius R_1 but are coated with an impenetrable sheath of polymer due to the chain units near the ionic groups. As a result, the radius of closest approach, R_{CA}, is greater than R_1. Other parameters obtained from the model analysis are V_p, the total volume of material per ionic aggregate (reciprocal of aggregate number density), and ρ_1, the electron density difference between the aggregates and the matrix. The modified Yarusso model employs the Percus–Yevick[43] total correlation function, as solved by Wertheim[44] and Thiele,[45] instead of the Fournet[46] three-body function originally proposed. Kinning and Thomas[47] have shown that the Percus–Yevick function yields better results than the Fournet function for diblock copolymers exhibiting a spherical morphology.

The Yarusso model produces good fits to the ionomer peak when applied to sulfonated polystyrene[42] and elastomeric polyurethane[48] ionomers, with physically satisfying parameters. However, it does not predict the observed intensity upturn at very low angle, so only data above 0.65 nm^{-1} were considered in the fits. Broze et al.[49] have reported observing two peaks in the SAXS patterns of carboxy-telechelic polybutadiene neutralized with Mg^{2+}, Ca^{2+}, and Ba^{2+}. From the positions of these peaks (q ratio of 1:2), they concluded that the ions aggregate into lamellae. Only a single peak is apparent in the SAXS patterns of the carboxy-telechelic polyisoprenes shown in Figure 5 and in the data of Williams et al.,[17] suggesting that if lamellae are present they are highly disordered. Moudden et al.[50] have studied the same carboxy-telechelic polybutadiene as Broze et al., neutralized with Na^+, K^+, and Cs^+, and observed only one small-angle peak. They suggest that the aggregates are bilayer disks with a diameter:thickness ratio of approximately 2; however, the scattering from an ensemble of such particles would be virtually indistinguishable from the scattering from an ensemble of equivalent spheres. Therefore, the modified Yarusso model seems suitable to analyze the present telechelic data.

Table II
Modified Yarusso Model Fit Parameters

cation	R_1, nm	R_{CA}, nm	V_p, nm^3	ρ_1, nm^{-3}	n
Ca^{2+}	1.05	1.94	190	49	25
Sr^{2+}	0.99	2.02	184	44	24
Ni^{2+}	0.90	2.00	131	63	17
Zn^{2+}	0.87	2.04	134	53	17
Cd^{2+}	0.86	2.02	135	56	17

The best-fit parameters of the SAXS data to the modified Yarusso model are given in Table II. First, note that the volume fraction of ionic aggregates, equal to $(4\pi/3)(R_1^3/V_p)$, is only 2.0–2.5% for these materials. Applying the empirical equation of Eilers and van Dijk, as quoted by Ferry,[32] shows that the filler effect in these materials leads to less than 7% modulus enhancement and thus cannot be the source of the 30–130% enhancement observed here.

The R_1 values for the Ca^{2+} and Sr^{2+} ionomers are larger than those for the Ni^{2+}, Zn^{2+}, and Cd^{2+} ionomers, suggesting that the aggregates in the former two materials contain larger numbers of ions. However, the size of the ionic aggregates is also influenced by the size of the neutralizing cation, any hydrocarbon incorporated into the aggregates, and any water absorbed from the atmosphere. Assuming that all the ions reside in aggregates, a more reliable indicator of the number of cations per ionic aggregate is V_p, the volume of material per aggregate. The value of this parameter is primarily determined by the ionomer peak position, rather than by nuances of peak shape, and is little affected by the factors just mentioned. In ionomers wherein the ionic sites are randomly distributed along the polymer backbone, a large fraction of the ionic groups may remain dispersed in the matrix[42] due to topological constraints imposed by the polymer chain. However, the monodispersity and well-defined placement of the ionic groups in these telechelic ionomers should allow for greater phase separation. Williams et al.[17] concluded that phase separation was virtually complete for their similar set of telechelics.

On the basis of the molecular weight, functionality, and neutralization level of these telechelics, there is an average of 0.13 ions/nm^3. Multiplying this factor by the V_p value yields the number of ions per aggregate, n, listed in Table II. There is a clear division in n between the Ca^{2+} and Sr^{2+} materials (n = 24–25) and the Ni^{2+}, Zn^{2+}, and Cd^{2+} materials (n = 17). Larger values of V_p and n indicate that the aggregation process has proceeded further for the Ca^{2+} and Sr^{2+} telechelics, forming larger aggregates. This will, in turn, lead to more trapped entanglements. As an example, imagine the coalescence of two neighboring aggregates; initially, some polymer chains would have one end in each aggregate, but after the two aggregates have merged, these chains become loops. It can be concluded that the higher small-strain tensile moduli observed for the Ca^{2+} and Sr^{2+} materials are due to a greater density of interlocking loops as a result of the larger aggregates in these materials.

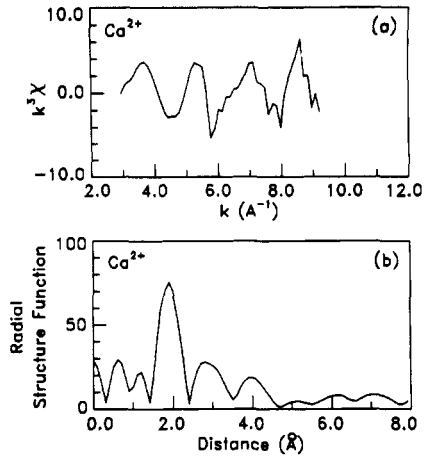

Figure 6. EXAFS data for the Ca^{2+} carboxy-telechelic polyisoprene: (a) $k^3\chi$ vs k; (b) radial structure function.

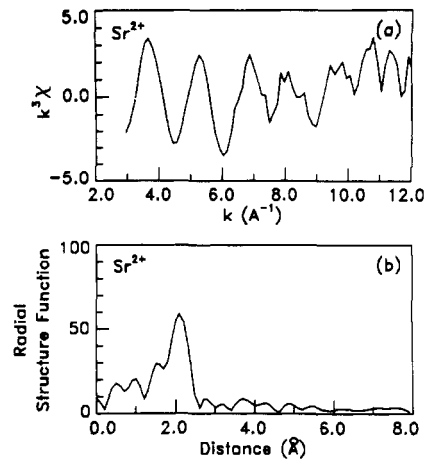

Figure 7. EXAFS data for the Sr^{2+} carboxy-telechelic polyisoprene: (a) $k^3\chi$ vs k; (b) radial structure function.

E. Extended X-ray Absorption Fine Structure (EXAFS). In order to estimate the cohesiveness of the ionic aggregates, we applied EXAFS spectroscopy to examine the coordination structure about the cation. The EXAFS signal is a modulation of the X-ray absorption coefficient on the high-energy side of an elemental absorption edge. The photoelectrons that are ejected by the absorbed X-rays can be backscattered by atoms coordinated to the absorbing atom; superposition of the outgoing and backscattered electron waves gives rise to an interference pattern. The EXAFS signal $\chi(k)$, where k is the photoelectron wave vector, contains information on the number N_j and type of atoms in coordination shell j, the distance R_j to this shell, and the static and vibrational disorder of the shell, measured as the Debye–Waller factor σ_j. To convert the EXAFS signal from wave vector to real space, it is Fourier transformed to yield the radial structure function, or RSF. Each nonartifactual peak in the RSF represents a distinct coordination shell; the peak positions are shifted slightly from the true shell distances by a phase shift ϕ_j that the photoelectron experiences in backscattering. Previous applications of EXAFS to ionomers[51-57] have revealed varying degrees of order within the ionic domains, ranging from highly ordered domains in ferric-neutralized carboxy-telechelic polybutadienes[57] to essentially no local order in domains of rubidium-neutralized sulfonated polystyrene.[54]

The EXAFS data were analyzed with single-electron single-scattering theory:[21]

$$\chi(k) = \sum_j \frac{N_j \gamma_j}{kR_j^2} f_j(k) \sin [2kR_j + \phi_j(k)] \exp(-2k^2\sigma_j^2) \quad (4)$$

where k is the wave vector defined as $k = (2\pi/h)[2m(E - E_0)]^{1/2}$ (where E is the incident X-ray energy), h is Planck's constant, and m is the mass of an electron. E_0 is approximately equal to the edge energy but is allowed to vary slightly to provide the best fit to the data and to correct for any errors in energy calibration.[58] γ_j accounts for the amplitude reduction due to inelastic scattering and is approximated as $\exp(-2R_j/\lambda)$, with λ defining a mean-free-path parameter. λ was obtained by analyzing model compounds of known structure and is assumed to be transferrable to other structures having the same coordination pairs. The model compounds used here were the 1:1 oxides CaO, SrO, NiO, ZnO, and CdO. All of these have the sodium chloride crystal structure,[59] except for ZnO, which has a pseudohexagonal structure ("zincite" structure).[60,61] These made particularly useful model compounds, as the first coordination shell is composed of M–O pairs and the second of M–M pairs, the two types needed for the analysis. $f_j(k)$ and $\phi_j(k)$ are the backscattering amplitude and phase-shift functions, respectively, which are characteristic of the types of atoms in shell j and the absorbing atom. The calculations of Teo and Lee[58] were used throughout for these functions. To correct for minor errors in the calculated phase shifts, the M–O and M–M distances determined by EXAFS were compared with the known crystallographic distances,[59,61] and the difference between the crystallographic and EXAFS values was added to the values determined for the telechelics. Errors

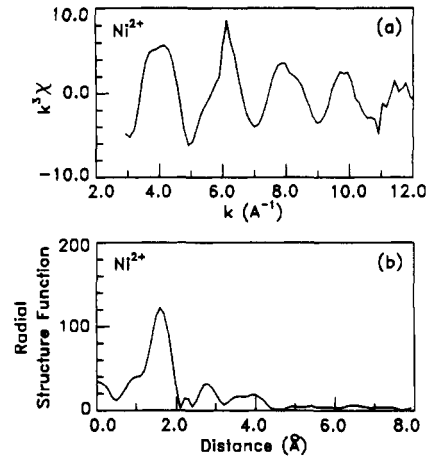

Figure 8. EXAFS data for the Ni^{2+} carboxy-telechelic polyisoprene: (a) $k^3\chi$ vs k; (b) radial structure function.

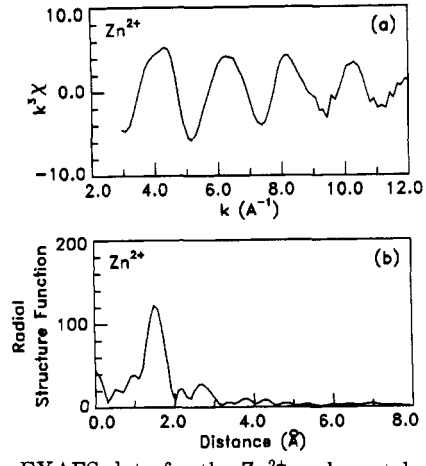

Figure 9. EXAFS data for the Zn^{2+} carboxy-telechelic polyisoprene: (a) $k^3\chi$ vs k; (b) radial structure function.

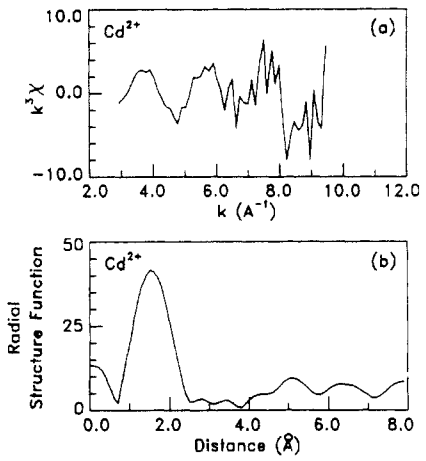

Figure 10. EXAFS data for the Cd^{2+} carboxy-telechelic polyisoprene: (a) $k^3\chi$ vs k; (b) radial structure function.

Table III
EXAFS Structural Parameters

cation	shell number (j)	shell element	R_j, Å	N_j	σ_j, Å	Q, %[a]
Ca^{2+}	1	O	2.40	5.5	0.05[b]	26.69[c]
	2	Ca	3.48	3.6	0.07[b]	
Sr^{2+}	1	O	2.58	5.1	0.082	3.63
Ni^{2+}	1	O	2.08	7.1	0.071	4.95
	2	Ni	3.09	1.4	0.086	2.82
Zn^{2+}	1	O	1.96	4.6	0.060	1.72
	2	Zn	2.97	0.9	0.098	3.94
Cd^{2+}	1	O	2.29	7.0	0.086	3.02

[a] The quality of fit, Q, is defined as the square root of the ratio of the sum of the squares of the residue to the sum of the squares of the data. [b] Held fixed during regression. [c] Q values for a simultaneous two-shell fit.

in the amplitude functions are automatically cancelled by using model compounds with the same coordination pairs.

The EXAFS data, both $\chi(k)$ and the RSF for each ionomer, are shown in Figures 6–10. Note that peaks below 1.5 Å in the RSF are artifacts of imperfect background subtraction and do not represent coordination shells. The Ca^{2+}, Ni^{2+}, and Zn^{2+} telechelics have more than one coordination shell visible in the RSF, while the other two telechelics have only one visible shell. To quantify these results, we computed the parameters for each of the first two shells, where visible; the results are listed in Table III. The R_j values are generally considered to be accurate to within 1%, while the N_j values are correct to within about 20%.[62,63] Note that the poorest data, in terms of signal-to-noise ratio and k-range, were obtained for the Ca^{2+} and Cd^{2+} telechelics. These elements have K edges near, respectively, the lower and upper energy limits available at CHESS. So that the regression routine would converge, it was necessary to fix the Debye–Waller factors σ_j for the two shells of the Ca^{2+} telechelic and the CaO model compound. In this range of σ_j, fortunately, it was found that variation in σ_j has only a minor effect on the determined values of R_j and N_j. Since the problems (including high values of the agreement factor Q) were identical for the Ca^{2+} telechelic and CaO, they do not reflect incorrect peak assignments but rather the difficulty in operating at such a low-energy absorption edge.

In all cases, the first peak arises from oxygen atoms while the second peak (where present) is due to metal atoms. This strongly suggests that the first shell is due to water molecules absorbed by the ionomer in handling, as hydrogen atoms are poor electron scatterers and not visible by EXAFS. While some of the oxygen atoms could be from carboxylate groups, the absence of a discernible carbon shell suggests that such species, if present, are in the minority. The coordination number for the first shell in each of the Ca^{2+}, Sr^{2+}, Ni^{2+}, and Cd^{2+} ionomers is within 20% of 6, the value for the oxide, so all four are likely to be octahedrally coordinated by oxygen. The value of 4.6 for the Zn^{2+} telechelic could reflect either four- or fivefold coordination; however, the Zn–O distance of 1.96 Å strongly implies tetrahedral coordination, as found by Pan et al. in a study of model compounds.[53]

As for the second shell, such metal–metal distances have been observed previously by EXAFS in nickel[51] and iron[52] neutralized Nafion ionomers. For such a well-defined M–M distance to be present, the two metal atoms must be somehow connected, such as by bridging through hydroxyl groups,[52] wherein the two metal atoms share oxygen atoms in their first coordination shells. The nature of the bridging oxygen is difficult to determine by EXAFS, however, since hydrogen atoms are not visible. Regardless of the nature of the bridge, such ionic "oligomers" form a more cohesive ionic aggregate, since pulling an ionic group from the aggregate would require disruption of these M–M distances. The coordination number of the second shell decreases in the order $Ca^{2+}(3.6) > Ni^{2+}(1.4) > Zn^{2+}(0.9) > Sr^{2+},Cd^{2+}(0)$. The same order is observed in the strain-hardening behavior, as shown by the Mooney–Rivlin plots in Figure 3; the Ca^{2+} telechelic exhibits marked strain hardening at approximately 50% elongation, the Ni^{2+} telechelic begins to harden near 100% elongation, and the other three ionomers show no strain-hardening behavior. This remarkable correlation strongly supports the hypothesis set forth earlier: stressed entanglements cannot relax in a material with tightly bound aggregates, causing strain hardening and subsequent sample failure, while those in materials with weakly bound aggregates can relax by ion hopping.

As a final note, because of the presence of water in the ionic aggregates, we cannot state conclusively which cation would produce an "inherently" tougher ionomer. It is possible that in the complete absence of water a different ordering in the mechanical properties would prevail, as the relative size and cohesiveness of the aggregates composed of different cations may be altered in the dry state. However, the general relationship between tensile behavior and aggregate size and cohesion should remain.

IV. Conclusions

A series of narrow-distribution carboxy-telechelic vinyl polyisoprenes of molecular weight 8000, neutralized with Ca^{2+}, Sr^{2+}, Ni^{2+}, Zn^{2+}, and Cd^{2+}, were examined by various techniques. By ^1H FTNMR, the microstructure of the polyisoprene chain was found to be 59% 3,4 addition, 41% 1,2 addition, and no 1,4 addition, while the glass transition temperatures of these elastomers lay in the range 15–19 °C. The small-strain tensile moduli of these materials were 30–130% higher than predicted based on the contribution of ionic aggregates acting as physical cross-links, with the Ca^{2+} and Sr^{2+} materials having higher moduli than the Ni^{2+}, Zn^{2+}, and Cd^{2+} telechelics. The modulus enhancement was attributed to entanglements, in the form of interlocking loops formed when both ends of a telechelic chain reside in the same aggregate. Small-angle X-ray scattering revealed that the Ca^{2+} and Sr^{2+} materials form larger aggregates, creating more trapped entanglements and raising the tensile moduli. Strain-hardening behavior was observed for the Ca^{2+} telechelic near 50% elongation and for the Ni^{2+} ionomer near 100% elongation but not in the other three materials. Extended X-ray absorption fine structure spectroscopy showed that the Ca^{2+} and Ni^{2+} materials have more cohesive ionic microdomains, as ev-

idenced by a pronounced metal–metal coordination shell. Therefore, ion hopping is more difficult in the Ca^{2+} and Ni^{2+} telechelics, causing the materials to strain-harden and break when the interlocking loops pull taut, whereas stressed entanglements in the Sr^{2+}, Zn^{2+}, and Cd^{2+} ionomers can relax by pulling ionic chain ends out of the aggregates.

Acknowledgment. We wish to thank Mr. Gregory Kalscheur for carrying out the DSC measurements. The help of Dr. Day-chyuan Lee in collecting the EXAFS data and of Dr. Janis L. C. Stevenson in using the SAXS equipment was also welcome. The staff of the Cornell High Energy Synchrotron Source (CHESS) of the Wilson Synchrotron Laboratory at Cornell University was invaluable in carrying out the EXAFS experiments. R.A.R. wishes to thank S. C. Johnson & Sons for a fellowship held while this work was performed. M.F. and R.J. are very much indebted to Service de la Programmation de la Politique Scientifique (SPPS, Brussels). Partial support of this research by the U.S. Department of Energy under Contract No. DE-AC02-81-ER10922 is gratefully acknowledged.

References and Notes

(1) Eisenberg, A.; King, M., Eds. *Ion Containing Polymers*; Halsted-Wiley: New York, 1975.
(2) *Ion in Polymers*; Eisenberg, A., Ed.; Advances in Chemistry 187; American Chemical Society: Washington, DC, 1980.
(3) Bazuin, C. G.; Eisenberg, A. *Ind. Eng. Chem. Prod. Res. Dev.* **1981**, *20*, 271.
(4) MacKnight, W. J.; Earnest, T. R. *Macromol. Rev.* **1981**, *16*, 41.
(5) *Structure and Properties of Ionomers*; Pinéri, M., Eisenberg, A., Eds.; NATO ASI Series C; D. Reidel: Boston, 1987; Vol. 198.
(6) Wilson, F. C.; Longworth, R.; Vaughan, D. J. *Polym. Prepr. (Am. Chem. Soc., Div. Polym. Chem.)* **1968**, *9*, 505.
(7) Eisenberg, A. *Macromolecules* **1970**, *3*, 147.
(8) Otocka, E. P.; Hellman, M. Y.; Blyler, L. L. *J. Appl. Phys.* **1969**, *40*, 4221.
(9) Pinéri, M.; Meyer, C.; Levelut, A. M.; Lambert, M. *J. Polym. Sci., Polym. Phys. Ed.* **1974**, *12*, 115.
(10) Jérôme, R.; Broze, G. *Rubber Chem. Technol.* **1985**, *58*, 223.
(11) Bagrodia, S.; Mohajer, Y.; Wilkes, G. L.; Storey, R. F.; Kennedy, J. P. *Polym. Bull.* **1982**, *8*, 281.
(12) Bagrodia, S.; Mohajer, Y.; Wilkes, G. L.; Storey, R. F.; Kennedy, J. P. *Polym. Bull.* **1983**, *9*, 174.
(13) Bagrodia, S.; Wilkes, G. L.; Kennedy, J. P. *Polym. Eng. Sci.* **1986**, *26*, 662.
(14) Broze, G.; Jérôme, R.; Teyssié, P. *Macromolecules* **1981**, *14*, 224.
(15) Broze, G.; Jérôme, R.; Teyssié, P. *Macromolecules* **1982**, *15*, 920.
(16) Broze, G.; Jérôme, R.; Teyssié, P. *Macromolecules* **1983**, *16*, 1771.
(17) Williams, C. E.; Russell, T. P.; Jérôme, R.; Horrion, J. *Macromolecules* **1986**, *19*, 2877.
(18) Tant, M. R.; Song, J. H.; Wilkes, G. L.; Horrion, J.; Jérôme, R. *Polymer* **1986**, *27*, 1815.
(19) Kratky, O.; Pilz, I.; Schmitz, P. J. *J. Colloid Interface Sci.* **1966**, *21*, 24.
(20) Sayers, D. E.; Stern, E. A.; Lytle, F. W. *Phys. Rev. Lett.* **1971**, *27*, 1024.
(21) Stern, E. A.; Sayers, D. E.; Lytle, F. W. *Phys. Rev. B: Solid State* **1975**, *11*, 4836.
(22) Lee, P. A.; Citrin, P. H.; Eisenberger, P.; Kincaid, B. M. *Rev. Mod. Phys.* **1981**, *53*, 769.
(23) Bovey, F. A. *High Resolution NMR of Macromolecules*; Academic: New York, 1972.
(24) Pham, Q.-T. *Polym. Lett.* **1970**, *8*, 723.
(25) Foucart, M.; Jérôme, R., unpublished data.
(26) Mooney, M. *J. Appl. Phys.* **1940**, *11*, 582.
(27) Rivlin, R. S. *Philos. Trans. R. Soc. London, A* **1948**, *241*, 379.
(28) Mark, J. E. *Rubber Chem. Technol.* **1975**, *48*, 495.
(29) Ward, T. C.; Tobolsky, A. V. *J. Appl. Polym. Sci.* **1967**, *11*, 2903.
(30) Sakamoto, K.; MacKnight, W. J.; Porter, R. S. *J. Polym. Sci., Polym. Phys. Ed.* **1970**, *8*, 277.
(31) Hara, M.; Eisenberg, A.; Storey, R. F.; Kennedy, J. P. In *Coulombic Interactions in Macromolecular Systems*; Eisenberg, A., Bailey, F. E., Eds.; *ACS Symposium Series 302*; American Chemical Society: Washington, DC, 1986.
(32) Ferry, J. D. *Viscoelastic Properties of Polymers*, 3rd ed.; Wiley: New York, 1980.
(33) Graessley, W. W. *Macromolecules* **1975**, *8*, 186.
(34) Flory, P. J. *J. Chem. Phys.* **1977**, *66*, 5720.
(35) Flory, P. J. *Principles of Polymer Chemistry*; Cornell University Press: Ithaca, NY, 1953; p 413.
(36) Kurata, M.; Tsunashima, Y.; Iwama, M.; Kamada, K. In *Polymer Handbook*, 2nd ed.; Brandrup, J., Immergut, E. H., Eds.; Wiley: New York, 1975.
(37) Forsman, W. C. *Macromolecules* **1982**, *15*, 1032.
(38) Dreyfus, B. *Macromolecules* **1985**, *18*, 284.
(39) Kumar, S.; Pinéri, M. *J. Polym. Sci., Polym. Phys. Ed.* **1986**, *24*, 1767.
(40) Lake, J. A. *Acta Crystallogr.* **1967**, *23*, 191.
(41) Porod, G. *Kolloid Z.* **1951**, *124*, 83.
(42) Yarusso, D. J.; Cooper, S. L. *Macromolecules* **1983**, *16*, 1871.
(43) Percus, J. K.; Yevick, G. *Phys. Rev.* **1958**, *110*, 1.
(44) Wertheim, M. S. *Phys. Rev. Lett.* **1963**, *10*, 321.
(45) Thiele, E. *J. Chem. Phys.* **1963**, *39*, 474.
(46) Fournet, G. *Acta Crystallogr.* **1951**, *4*, 293.
(47) Kinning, D. J.; Thomas, E. L. *Macromolecules* **1984**, *17*, 1712.
(48) Ding, Y. S. Ph.D. Thesis, University of Wisconsin—Madison, 1986.
(49) Broze, G.; Jérôme, R.; Teyssié, P.; Gallot, B. *J. Polym. Sci., Polym. Lett. Ed.* **1981**, *19*, 415.
(50) Moudden, A.; Levelut, A. M.; Pinéri, M. *J. Polym. Sci., Polym. Phys. Ed.* **1977**, *15*, 1707.
(51) Pan, H. K.; Yarusso, D. J.; Knapp, G. S.; Cooper, S. L. *J. Polym. Sci., Polym. Phys. Ed.* **1983**, *21*, 1389.
(52) Pan, H. K.; Yarusso, D. J.; Knapp, G. S.; Pinéri, M.; Meagher, A.; Coey, J. M. D.; Cooper, S. L. *J. Chem. Phys.* **1983**, *79*, 4736.
(53) Pan, H. K.; Knapp, G. S.; Cooper, S. L. *Colloid Polym. Sci.* **1984**, *262*, 734.
(54) Yarusso, D. J.; Ding, Y. S.; Pan, H. K.; Cooper, S. L. *J. Polym. Sci., Polym. Phys. Ed.* **1984**, *22*, 2073.
(55) Ding, Y. S.; Yarusso, D. J.; Pan, H. K.; Cooper, S. L. *J. Appl. Phys.* **1984**, *56*, 2396.
(56) Jérôme, R.; Vlaic, G.; Williams, C. E. *J. Phys. Lett.* **1983**, *44*, 717.
(57) Meagher, A.; Coey, J. M. D.; Belakhovsky, M.; Pinéri, M.; Jérôme, R.; Vlaic, G.; Williams, C.; Dang, N. V. *Polymer* **1986**, *27*, 979.
(58) Teo, B. K.; Lee, P. A. *J. Am. Chem. Soc.* **1979**, *101*, 2815.
(59) *Crystal Data: Determinative Tables*, 3rd ed.; Donnay, J. D. H.; Ondik, H. M., Eds.; National Bureau of Standards: Washington, DC, 1973; Vol. II.
(60) Wyckoff, R. W. G. *Crystal Structures*; Interscience: New York, 1948.
(61) Abrahams, S. C.; Bernstein, J. L. *Acta Crystallogr., Sect. B: Struct. Crystallogr. Cryst. Chem.* **1969**, *25*, 1233.
(62) Lengler, B.; Eisenberger, P. *Phys. Rev. B: Condens. Matter* **1980**, *22*, 4507.
(63) Stern, E. A.; Kim, K. *Phys. Rev. B: Condens. Matter* **1981**, *23*, 781.